Research article

Optimizing computed tomography image reconstruction for focal hepatic lesions: Deep learning image reconstruction vs iterative reconstruction

Varin Jaruvongvanich [a], Kobkun Muangsomboon [a], Wanwarang Teerasamit [a], Voraparee Suvannarerg [a], Chulaluk Komoltri [b], Sastrawut Thammakittiphan [a], Wimonrat Lornimitdee [a], Witchuda Ritsamrej [a], Parinya Chaisue [a], Napapong Pongnapang [c], Piyaporn Apisarnthanarak [a,*]

[a] Department of Radiology, Faculty of Medicine Siriraj Hospital, Mahidol University, Bangkok, Thailand
[b] Division of Research and Development, Faculty of Medicine Siriraj Hospital, Mahidol University, Bangkok, Thailand
[c] Department of Radiological Technology, Faculty of Medical Technology, Mahidol University, Bangkok, Thailand

ARTICLE INFO

ABSTRACT

Background: Deep learning image reconstruction (DLIR) is a novel computed tomography (CT) reconstruction technique that minimizes image noise, enhances image quality, and enables radiation dose reduction. This study aims to compare the diagnostic performance of DLIR and iterative reconstruction (IR) in the evaluation of focal hepatic lesions.

Methods: We conducted a retrospective study of 216 focal hepatic lesions in 109 adult participants who underwent abdominal CT scanning at our institution. We used DLIR (low, medium, and high strength) and IR (0 %, 10 %, 20 %, and 30 %) techniques for image reconstruction. Four experienced abdominal radiologists independently evaluated focal hepatic lesions based on five qualitative aspects (lesion detectability, lesion border, diagnostic confidence level, image artifact, and overall image quality). Quantitatively, we measured and compared the level of image noise for each technique at the liver and aorta.

Results: There were significant differences ($p < 0.001$) among the seven reconstruction techniques in terms of lesion borders, image artifacts, and overall image quality. Low-strength DLIR (DLIR-L) exhibited the best overall image quality. Although high-strength DLIR (DLIR-H) had the least image noise and fewest artifacts, it also had the lowest scores for lesion borders and overall image quality. Image noise showed a weak to moderate positive correlation with participants' body mass index and waist circumference.

Conclusions: The optimal-strength DLIR significantly improved overall image quality for evaluating focal hepatic lesions compared to the IR technique. DLIR-L achieved the best overall image quality while maintaining acceptable levels of image noise and quality of lesion borders.

1. Background

Computed tomography (CT) is essential for lesion diagnosis, treatment planning, follow-up, and complication assessment. Various CT image reconstruction techniques have been proposed to improve image quality and reduce scan time [1]. However, high-quality CT images inevitably come with high radiation exposure. This poses a potential cancer risk, particularly for young patients or those requiring frequent or long-term follow-up CT scans [2–5]. Abdominal CT typically has an estimated effective dose of approximately 10 mSv or within the range of 3.5–25 mSv [5]. Radiation exposure of 10 mSv is associated with an average lifetime risk of 0.1 % for cancer incidence and 0.05 % for mortality [6].

Radiation exposure during CT examinations is influenced by device factors (scanner generation, detector array), CT protocol factors (multiphase acquisition, tube current, tube voltage, scan time, scan coverage, scan pitch), and patient factors (age, sex, body habitus) [2,6–9]. Several techniques have been proposed for radiation dose optimization, such as patient selection, reducing the number of CT phase acquisitions and scan coverage, and minimizing tube current and peak kilovoltage [6–11]. However, these approaches have trade-offs, including decreased image quality and increased noise [1]. These factors predominantly affect the visibility of low-contrast lesions such as those in the liver, spleen, or pancreas [12–15]. Over the past few decades, novel image reconstruction techniques have been developed to replace the original filtered back-projection (FBP) technique [15]. Two prominent techniques are iterative reconstruction (IR) [15–23] and deep learning image reconstruction (DLIR) [24–27], which aim to reduce image noise and improve quality [8,28].

Iterative reconstruction, as one of the currently mainstream CT reconstruction techniques, provides less image noise than the conventional FBP [1]. However, the major drawback of IR is providing super-smooth image appearances with less sharp border. Some radiologists describe the CT images reconstructed by IR technique as plastic-like or unnatural [23].

The DLIR technique [1,23,26,29] utilizes artificial intelligence (AI) and a supercomputing system trained on multiple image reconstruction sets to generate CT images. Two well-accepted versions currently available are TrueFidelity (GE Healthcare) and Advanced Intelligent Clear-IQ Engine (AiCE; Canon Medical Systems). Recent studies have demonstrated the superiority of TrueFidelity over the adaptive statistical iterative reconstruction-V (ASiR-V) technique (also owned by GE Healthcare) in both phantom and real patient scenarios. These investigations showed that DLIR effectively reduces noise, enhances image quality, and improves lesion detectability [27,30–35].

This study compared the diagnostic performance of the DLIR (TrueFidelity) and statistical IR (ASiR-V) techniques in the assessment of focal hepatic lesions from both qualitative and quantitative perspectives.

2. Methods

This retrospective single-center study took place in a 2200-bed university hospital in central Thailand. Institutional review board approval was obtained, and written informed consent was waived due to the study's retrospective design.

2.1. Participants

The study included adult patients (≥18 years old) who underwent contrast-enhanced abdominal CT at the institution between July and November 2022. Participants with at least one focal hepatic lesion measuring ≥1 cm were eligible. Patients were excluded if they
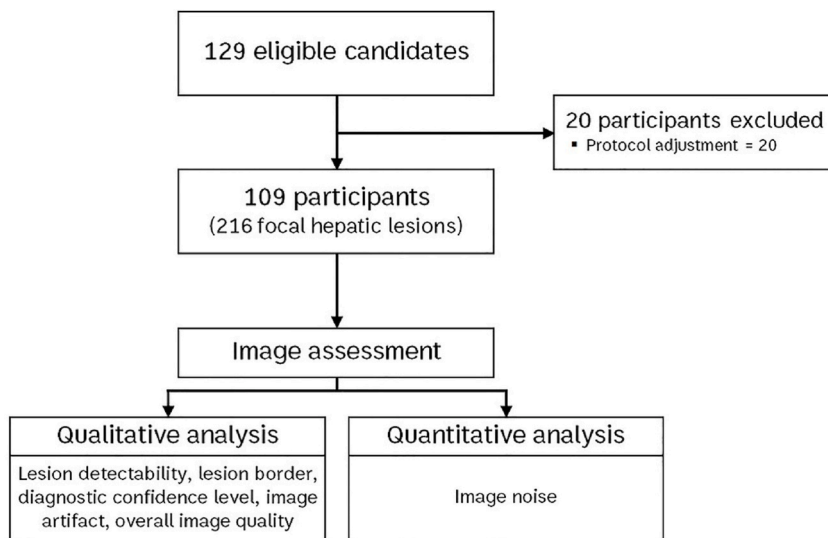

Fig. 1. The study flow chart of the included participants and image assessment.

had incomplete medical records, significant respiratory motion or beam hardening artifacts impacting image quality of the original CT image data set, or protocol adjustments (e.g., dual-energy CT). The study population consisted of 109 participants with 216 focal hepatic lesions (Fig. 1). One investigator (VJ) recorded the age, sex, body weight, height, body mass index (BMI), waist circumference, and underlying diseases of each participant.

2.2. CT examination and image reconstruction

All participants underwent contrast-enhanced abdominal CT using two 256-slice CT scanners (Revolution Apex and Revolution CT; GE Healthcare, Milwaukee, WI, USA). Breath-holding instructions were provided during the scan, which covered at least the upper abdomen with a slice collimation of 1.25 mm for both scanners. Oral or rectal contrast administration varied with patients' clinical indications. All participants were administered an intravenous injection of nonionic iodinated contrast media (320–370 mgI/mL) at a dose of 2 mL per kg body weight, followed by a 20 mL saline flush via a power injector (3 mL/s). The portovenous phase (80-s delay after IV contrast administration) was obtained in all participants. Additional precontrast, arterial (40-s delay), or delayed (5- to 10-min delay) phases were acquired as necessary. A standard optimized radiation dose protocol was employed for participants with a body weight <75 kg, utilizing a peak kilovoltage of 120 kVp, tube current of 250 mA, rotation time of 0.5 s, and pitch of 0.992:1. For participants whose body weight was ≥75 kg, suitable adjustments were made to the tube current (up to 450 mA). The volume CT dose index ($CTDI_{vol}$) was recorded for each participant.

Raw data from the portovenous image set were reconstructed using 7 techniques at the CT scanner console by senior CT technologists (ST and WL). The techniques comprised 3 DLIR (TrueFidelity) techniques with low (DLIR-L), medium (DLIR-M), and high (DLIR-H) strengths, as well as 4 levels of IR (ASiR-V) techniques (0 %, 10 %, 20 %, and 30 %; Fig. 2). Each participant obtained 7 sets of CT images using these reconstruction protocols. The reconstructed image sets were anonymized by renaming them from "Recon 1" to "Recon 7" using a computer-generated random technique that was unique to each participant. Subsequently, all 7 CT image sets for each participant were sent to the Picture Archiving and Communication System (PACS) for review.

2.3. Image assessment

One to three hepatic lesions (≥1 cm) per participant were selected by a nonreader researcher (VJ) for subsequent review. In patients with more than three lesions, the three lesions with the largest diameters were chosen. The selected hepatic lesion(s) were annotated in the Recon 1 image set as a reference for the readers.

2.3.1. Qualitative analyses

Four board-certified abdominal radiologists (PA, KM, WT, VS) with 26, 26, 20, and 17 years of experience in abdominal CT evaluation, respectively, independently reviewed the 7 image sets for each participant. They were aware that each participant had undergone 7 reconstruction techniques, including various DLIR strengths and ASIR-V percentages, but they were blinded to the specific reconstruction techniques used (Recon 1 to Recon 7). The readers had access to clinical data, previous imaging studies, and other available CT phase acquisitions to simulate real clinical practice. They were able to freely scroll, zoom, and adjust window settings. The qualitative evaluations encompassed 5 aspects (Table 1).

2.3.2. Quantitative analyses

One investigator (VJ) performed the quantitative analyses by measuring image noise (standard deviation of CT attenuation, HU) at four locations in all 7 reconstructed image sets. Circular regions of interest (ROIs) were carefully placed at three locations in the liver (right anterior, right posterior, and left hepatic lobes) and one in the aorta (Fig. 3). The hepatic ROIs were selected from the most homogeneous-enhancing areas away from hepatic vessels, bile ducts, and hepatic space-occupying lesions. In cases of previous hepatic surgery or anatomical variations, the ROIs were placed in three different areas within the visualized liver. The aortic ROI was positioned at the central part of the aorta to avoid atherosclerotic plaques. The liver and aortic ROIs had size ranges of 100–150 mm^2 (mean ± SD, 124.9 ± 4.6 mm^2) and 60–100 mm^2 (mean ± SD, 80.2 ± 5.8 mm^2), respectively. The mean image noise measured from
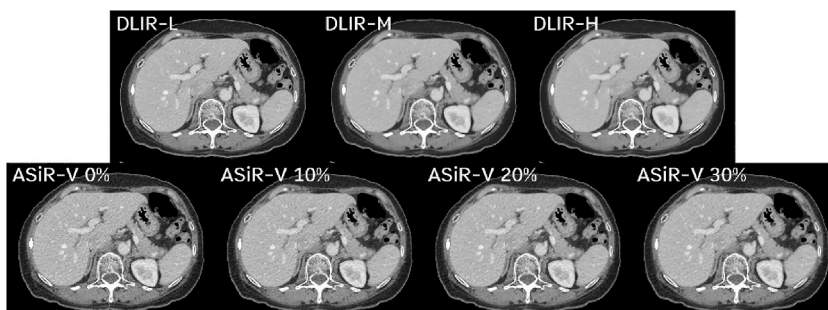

Fig. 2. Comparison of 7 reconstructed image sets using DLIR and ASiR-V techniques at various strengths.

Table 1
Details of the five aspects of qualitative assessment.

The Qualitative Assessment	Score
Lesion detectability	0 = Undetectable
	1 = Detectable
Lesion border	1 = Ill-defined border; significant effect to image interpretation
	2 = Less sharp border; no significant effect to image interpretation
	3 = Sharp border
Diagnostic confidence level	0 = Not confident to give diagnosis
	1 = Confident to give diagnosis
Image artifact	1 = Yes; significant effect to image interpretation
	2 = Yes; no significant effect to image interpretation
	3 = None
Overall image quality	1 = Unacceptable, unable for image interpretation
	2 = Poor, interfere image interpretation
	3 = Average, with possible image interpretation
	4 = Good
	5 = Excellent

Remarks: Lesion detectability, lesion border, and diagnostic confidence level were evaluated per lesion basis, but image artifact and overall image quality were evaluated per reconstructed image set basis.
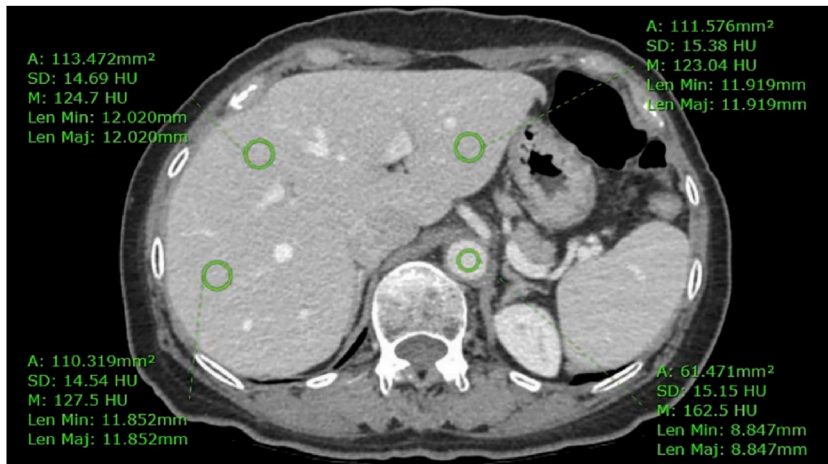
Fig. 3. Measurement of image noise at the aorta (single ROI) and the liver (three ROIs at right anterior, right posterior, and left hepatic lobes).

the three hepatic ROIs was calculated for each reconstructed image set.

2.4. Statistical analyses

Descriptive statistics summarized the demographic and clinical data (age, sex, BMI, waist circumference, underlying disease, $CTDI_{vol}$, and focal hepatic lesion details).

To compare the seven reconstruction techniques, Cochran's Q test was used for binary assessments (lesion detectability and diagnostic confidence level). Friedman's test was employed for ordinal variables (lesion border, image artifact, and overall image quality) to compare the techniques among each reader and all readers (using the mean score of the four readers). Multivariate tests evaluated the differences in image noise among the techniques. Pearson's correlation coefficient (r) was used to calculate the correlation between image noise and each of BMI and waist circumference, with interpretations as follows: 0–0.1 (negligible), 0.1–0.39 (weak), 0.4–0.69 (moderate), 0.7–0.89 (strong), and 0.9–1.0 (very strong) [36].

The analyses were performed using IBM SPSS Statistics, version 29 (IBM Corp, Armonk, NY, USA). Significant results were defined as those with two-sided *p* values less than 0.05.

3. Results

3.1. Participants

The demographic and clinical data, including the $CTDI_{vol}$, for the 109 participants are summarized in Table 2. The 216 hepatic lesions were categorized as follows: cystic lesions (74, 34.3 %), hemangioma/vascular lesions (14, 6.5 %), benign/probably benign

lesions (4, 1.9 %), hepatocellular carcinoma (12, 5.6 %), other primary malignant tumors (7, 3.2 %), metastases (64, 29.6 %), posttreatment lesions (36, 16.7 %), calcification (1, 0.5 %), and indeterminate lesions (4, 1.9 %). The lesion sizes ranged from 1 cm to 15.3 cm, with a mean size of 2.9 ± 2.47 cm. Among the lesions, 148 (68.5 %) were smaller than 3 cm (1–2.9 cm), while 68 (31.5 %) were 3 cm or larger.

3.2. Image assessment

3.2.1. Qualitative analyses

Table 3 presents the details of the 5 aspects analyzed in the qualitative assessment: lesion detectability, lesion border, diagnostic confidence level, image artifact, and overall image quality.

There were no significant differences in the lesion detectability and diagnostic confidence levels of the seven reconstruction techniques for all four readers. However, there were significant differences in the scores for lesion borders, image artifacts, and overall image quality among the techniques for all reviewers ($p < 0.001$). Some variations in scores were noted among readers based on their preferences and opinions. Nevertheless, the scores from all readers (mean score from four readers) indicated that increasing the strength of DLIR or IR resulted in images with fewer sharp borders and artifacts.

The overall image quality scores ranged from 2 to 5 for each reader, with only one reader assigning a score of 2 in a single case. Among the seven reconstruction techniques, DLIR-L achieved the highest mean scores for all readers.

3.2.2. Quantitative analyses

Descriptive statistics of mean image noise measured at the liver and aorta for the seven image reconstruction techniques are detailed in Fig. 4. There were significant differences in image noise among the techniques at both the liver and aorta ($p < 0.001$). Increasing the strength of DLIR or the percentage of IR led to lower image noise. The DLIR technique exhibited lower image noise than the ASiR-V technique.

Table 4 presents the Pearson's correlation coefficients (r) between image noise and two variables: BMI and waist circumference. Both liver and aorta image noise showed a weak to moderate positive correlation with BMI and waist circumference, with waist circumference showing a slightly stronger correlation.

4. Discussion

To optimize the radiation dose without compromising image quality, novel CT reconstruction techniques have been proposed. DLIR is one such technique that reduces image noise, allowing for a potential reduction in radiation dose [37–43]. This is particularly beneficial in certain clinical situations, for example, oncologic patients requiring regular follow-up or pediatric patients. In a study by Cao et al., DLIR demonstrated a reduction in radiation dose of up to 76 % [37]. TrueFidelity, the vendor-specific DLIR in our study, utilizes a deep neural network-based engine trained with high-quality filtered back-projection data, resulting in excellent images with suppressed noise [44].

Consistent with previous studies [30,31,42,45,46], our study showed that DLIR achieved lower image noise than the IR technique. However, excessively reducing image noise may lead to an unnaturally smooth image, adversely affecting image quality due to the loss of spatial resolution and blurred borders, as supported by some researches [30,46–48]. This issue was evident in our study, where the DLIR-H technique received the lowest overall image quality score, while DLIR-L achieved the best score in overall image quality.

Our findings align with previous studies [30,32,38,48,49] that reported that higher DLIR or IR strength leads to reduced image noise. We also observed a weak to moderate positive correlation between image noise and both BMI and waist circumference, consistent with prior studies [50,51]. In overweight or obese patients, increased body circumference or thickness hinders photon penetration, resulting in elevated image noise [52,53].

Our study showed that as the strength of DLIR and IR increased, there was a tendency for less-sharp borders. This can be attributed

Table 2
Demographic and clinical data of 109 participants, including CTDI$_{vol}$.

| Patient Data	Number (%)
Age (years)	* 65.0 ± 11.2 (34–87)
Gender:	
Female	60 (55.0)
Male	49 (45.0)
BMI ** (kg/m^2)	* 23.6 ± 4.3 (16.4–39.7)
Waist circumference (cm)	* 84.0 ± 10.5 (66–121)
Underlying diseases	
Cirrhosis	25 (22.9)
Chronic hepatitis B infection	14 (12.8)
Chronic hepatitis C infection	6 (5.5)
CTDI$_{vol}$ *** (mGy)	* 9.07 ± 1.33 (5.9–15.5)

Remarks: * Mean $\pm$ SD (range), ** BMI = Body mass index, *** CTDI$_{vol}$ = Volume CT dose index.

Table 3
Qualitative analysis of 7 image reconstruction techniques in 5 aspects.

A) Lesion detectability (0 = undetectable, 1 = detectable)

Reconstruction Techniques	Lesion Detectability: number (%)			
	Reader 1	Reader 2	Reader 3	Reader 4
DLIR-L	216 (100)	214 (99.1)	216 (100)	216 (100)
DLIR-M	216 (100)	214 (99.1)	216 (100)	216 (100)
DLIR-H	216 (100)	214 (99.1)	216 (100)	216 (100)
ASiR-V 0 %	216 (100)	214 (99.1)	216 (100)	216 (100)
ASiR-V 10 %	216 (100)	214 (99.1)	216 (100)	216 (100)
ASiR-V 20 %	216 (100)	214 (99.1)	216 (100)	216 (100)
ASiR-V 30 %	216 (100)	214 (99.1)	216 (100)	216 (100)
p-value	1.000	1.000	1.000	1.000

B) Lesion border (1 = ill-defined border, 2 = less sharp border, 3 = sharp border)

Reconstruction Techniques	Lesion Border: mean ± SD				
	Reader 1	Reader 2	Reader 3	Reader 4	All readers
DLIR-L	2.57 ± 0.58	2.74 ± 0.53	2.69 ± 0.52	3.00 ± 0	2.75 ± 0.36
DLIR-M	2.53 ± 0.60	2.71 ± 0.55	2.72 ± 0.50	2.93 ± 0.26	2.72 ± 0.39
DLIR-H	2.45 ± 0.61	2.62 ± 0.61	2.72 ± 0.50	2.74 ± 0.44	2.63 ± 0.44
ASiR-V 0 %	2.64 ± 0.55	2.73 ± 0.52	2.67 ± 0.55	3.00 ± 0.07	2.76 ± 0.36
ASiR-V 10 %	2.62 ± 0.56	2.75 ± 0.51	2.67 ± 0.55	3.00 ± 0	2.76 ± 0.36
ASiR-V 20 %	2.63 ± 0.55	2.75 ± 0.51	2.67 ± 0.54	3.00 ± 0	2.76 ± 0.35
ASiR-V 30 %	2.61 ± 0.56	2.73 ± 0.53	2.68 ± 0.54	3.00 ± 0	2.75 ± 0.36
p-value	<0.001	<0.001	<0.001	<0.001	<0.001

C) Diagnostic confidence level (0 = not confident to give diagnosis, 1 = confident to give diagnosis)

Reconstruction Techniques	Diagnostic Confidence Level: Number (%)			
	Reader 1	Reader 2	Reader 3	Reader 4
DLIR-L	180 (83.3)	209 (96.8)	211 (97.7)	216 (100)
DLIR-M	180 (83.3)	207 (95.8)	211 (97.7)	216 (100)
DLIR-H	180 (83.3)	206 (95.4)	211 (97.7)	216 (100)
ASiR-V 0 %	180 (83.3)	208 (96.3)	211 (97.7)	216 (100)
ASiR-V 10 %	180 (83.3)	207 (95.8)	211 (97.7)	216 (100)
ASiR-V 20 %	180 (83.3)	208 (96.3)	211 (97.7)	216 (100)
ASiR-V 30 %	180 (83.3)	208 (96.3)	211 (97.7)	216 (100)
p-value	1.000	0.353	1.000	1.000

D) Image artifact (1 = yes, significant effect, 2 = yes, no significant effect, 3 = none)

Reconstruction Techniques	Image Artifact: mean ± SD				
	Reader 1	Reader 2	Reader 3	Reader 4	All readers
DLIR-L	2.97 ± 0.21	2.95 ± 0.21	2.99 ± 0.10	3.00 ± 0	2.98 ± 0.09
DLIR-M	2.98 ± 0.14	2.97 ± 0.16	3.00 ± 0	3.00 ± 0	2.99 ± 0.06
DLIR-H	2.98 ± 0.14	2.99 ± 0.10	3.00 ± 0	3.00 ± 0	2.99 ± 0.05
ASiR-V 0 %	2.55 ± 0.52	2.61 ± 0.49	2.31 ± 0.47	2.61 ± 0.49	2.52 ± 0.30
ASiR-V 10 %	2.70 ± 0.48	2.79 ± 0.41	2.33 ± 0.47	2.83 ± 0.38	2.66 ± 0.27
ASiR-V 20 %	2.73 ± 0.46	2.88 ± 0.33	2.44 ± 0.50	2.97 ± 0.16	2.76 ± 0.22
ASiR-V 30 %	2.78 ± 0.44	2.87 ± 0.34	2.51 ± 0.50	2.96 ± 0.19	2.78 ± 0.22
p-value	<0.001	<0.001	<0.001	<0.001	<0.001

E) Overall image quality (1 = unacceptable, 2 = poor, 3 = average, 4 = good, 5 = excellent)

Reconstruction Techniques	Overall Image Quality: mean ± SD				
	Reader 1	Reader 2	Reader 3	Reader 4	All readers
DLIR-L	4.96 ± 0.23	4.02 ± 0.27	4.93 ± 0.35	4.98 ± 0.14	4.72 ± 0.15
DLIR-M	4.92 ± 0.31	4.01 ± 0.25	4.95 ± 0.32	4.88 ± 0.33	4.69 ± 0.18
DLIR-H	4.27 ± 0.46	3.83 ± 0.42	4.95 ± 0.32	4.24 ± 0.45	4.32 ± 0.24
ASiR-V 0 %	4.56 ± 0.52	3.95 ± 0.39	4.23 ± 0.50	4.92 ± 0.28	4.41 ± 0.27
ASiR-V 10 %	4.70 ± 0.48	3.96 ± 0.36	4.26 ± 0.50	4.96 ± 0.19	4.47 ± 0.25
ASiR-V 20 %	4.70 ± 0.48	3.98 ± 0.33	4.36 ± 0.55	5.00 ± 0	4.51 ± 0.26
ASiR-V 30 %	4.76 ± 0.45	4.02 ± 0.27	4.43 ± 0.55	5.00 ± 0	4.55 ± 0.23
p-value	<0.001	<0.001	<0.001	<0.001	<0.001

Remarks: DLIR-L, DLIR-M, DLIR-H = deep learning image reconstruction at low, medium, and high strengths; ASiR-V = adaptive statistical iterative reconstruction-V at 0 %, 10 %, 20 %, and 30 %.
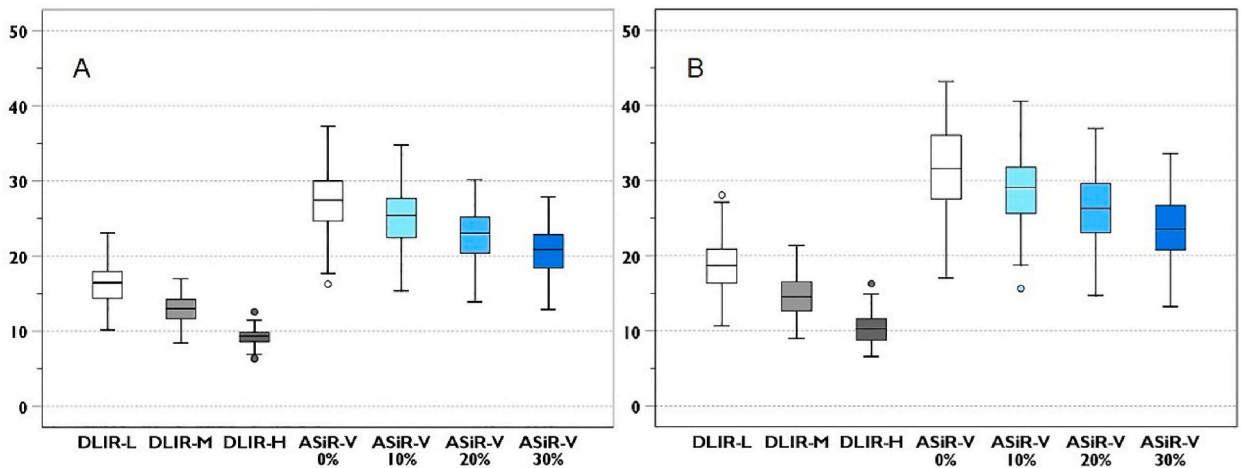
Fig. 4. Box plots depicting image noise (HU) across 7 image reconstruction techniques (*p*-value <0.001). A: Mean image noise measured at the liver from 3 hepatic ROIs. B: Image noise measured at the aorta.

Table 4

Pearson's correlation coefficient (r) between image noise and both BMI and waist circumference.

Reconstruction Techniques	Image Noises (Liver)		Image Noises (Aorta)	
	BMI	Waist Circumference	BMI	Waist Circumference
DLIR-L	0.511	0.606	0.340	0.506
DLIR-M	0.472	0.524	0.312	0.469
DLIR-H	0.357	0.428	0.246	0.399
ASiR-V 0 %	0.463	0.595	0.358	0.506
ASiR-V 10 %	0.467	0.592	0.314	0.492
ASiR-V 20 %	0.508	0.620	0.353	0.494
ASiR-V 30 %	0.500	0.637	0.330	0.478

Remarks: BMI = body mass index; DLIR-L, DLIR-M, DLIR-H = deep learning image reconstruction at low, medium, and high strengths, respectively; ASiR-V = adaptive statistical iterative reconstruction-V.

to the reduction in image noise and the resulting smoother appearance of the images. In our study, DLIR showed a less-sharp border than IR and received a better score for reducing image artifacts. However, our findings differ from Jensen et al. [30], who reported significantly improved lesion conspicuity with DLIR than with 30 % ASiR-V. In their study, DLIR-H achieved the highest score for lesion conspicuity, followed by DLIR-M and DLIR-L. A higher score for lesion border indicated improved lesion conspicuity against the hepatic background; this aids lesion detection in the liver, which is well known as a low-contrast organ [12–15]. In our study, DLIR-H received the lowest score in the lesion border aspect, probably related to its unnaturally smooth images. Despite providing the least image noise and fewest artifacts, DLIR-H achieved the lowest score for overall image quality.

Lesion detectability and diagnostic confidence level were similar among the seven reconstruction techniques, although slight variations were observed among readers. This may be attributed to the design of our study, which allowed readers access to clinical data, prior imaging studies, and other CT phase acquisitions, simulating real-world clinical practice. Our findings support the practicality of DLIR in clinical settings compared to commercially available IR.

Our study demonstrated that DLIR-L is the optimal reconstruction technique, offering the best overall image quality and producing an optimally smooth image while maintaining acceptable levels of image noise, artifacts, and lesion borders.

This retrospective study had limitations. First, it was conducted at a single institution in central Thailand. Second, it was also vendor-specific (GE Healthcare) with a focus on hepatic lesions ≥1 cm in size. Third, the significant proportion of the lesions in this study were cystic lesions, which had sharp border and were easily detected and diagnosed. Hence, further prospective study performed in several hospitals and utilizing several CT vendors should be designed with an emphasis on more solid and/or smaller hepatic lesions. These would provide additional information and confirm its generalizability and clinical applicability. Additionally, image noise measurements in our study were limited to the liver and aorta regions. Finally, although the readers were blinded to the CT reconstruction techniques, they were not blinded to other clinical information, prior imaging studies, or other CT phase acquisitions.

5. Conclusions

In summary, DLIR with optimal strength significantly improved overall image quality for evaluating focal hepatic lesions compared to the statistical IR technique. DLIR-L demonstrated the best overall image quality while maintaining image noise, artifacts, and lesion

borders within acceptable levels.

Ethics approval and consent to participate

This study was reviewed and approved by the Siriraj Institutional Review Board (IRB) with certificate of approval (COA) no. Si 394/2022. The written informed consent was waived due to the study's retrospective design and minimal risk involved.

Consent for publication

Not applicable.

Availability of data and materials

The datasets used and/or analyzed in this current study are not publicly available due to reasons of patients' privacy and confidentiality, but will be available upon reasonable request.

CRediT authorship contribution statement

Varin Jaruvongvanich: Writing – review & editing, Writing – original draft, Validation, Methodology, Investigation, Formal analysis, Data curation, Conceptualization. **Kobkun Muangsomboon:** Validation, Investigation. **Wanwarang Teerasamit:** Validation, Investigation. **Voraparee Suvannarerg:** Validation, Investigation. **Chulaluk Komoltri:** Writing – review & editing, Validation, Formal analysis. **Sastrawut Thammakittiphan:** Resources, Investigation, Data curation. **Wimonrat Lornimitdee:** Resources, Investigation, Data curation. **Witchuda Ritsamrej:** Resources, Investigation. **Parinya Chaisue:** Resources, Investigation. **Napapong Pongnapang:** Writing – review & editing. **Piyaporn Apisarnthanarak:** Writing – review & editing, Writing – original draft, Validation, Supervision, Methodology, Investigation, Formal analysis, Conceptualization.

Declaration of competing interest

The authors declare that they have no known competing financial interests or personal relationships that could have appeared to influence the work reported in this paper.

References

[1] M.J. Willemink, P.B. Noël, The evolution of image reconstruction for CT—from filtered back projection to artificial intelligence, Eur. Radiol. 29 (5) (2019) 2185–2195.
[2] D.J. Brenner, E.J. Hall, Computed tomography–an increasing source of radiation exposure, N. Engl. J. Med. 357 (22) (2007) 2277–2284.
[3] D. Brenner, C. Elliston, E. Hall, W. Berdon, Estimated risks of radiation-induced fatal cancer from pediatric CT, AJR Am. J. Roentgenol. 176 (2) (2001) 289–296.
[4] A. Berrington de González, S. Darby, Risk of cancer from diagnostic X-rays: estimates for the UK and 14 other countries, Lancet 363 (9406) (2004) 345–351.
[5] J.M. Albert, Radiation risk from CT: implications for cancer screening, AJR Am. J. Roentgenol. 201 (1) (2013) W81–W87.
[6] L. Yu, X. Liu, S. Leng, J.M. Kofler, J.C. Ramirez-Giraldo, M. Qu, J. Christner, J.G. Fletcher, C.H. McCollough, Radiation dose reduction in computed tomography: techniques and future perspective, Imag. Med. 1 (1) (2009) 65–84.
[7] R.V. Gottumukkala, M.K. Kalra, A. Tabari, A. Otrakji, M.S. Gee, Advanced CT techniques for decreasing radiation dose, reducing sedation requirements, and optimizing image quality in children, Radiographics 39 (3) (2019) 709–726.
[8] W.W. Mayo-Smith, A.K. Hara, M. Mahesh, D.V. Sahani, W. Pavlicek, How I do it: managing radiation dose in CT, Radiology 273 (3) (2014) 657–672.
[9] A.K. Hara, C.V. Wellnitz, R.G. Paden, W. Pavlicek, D.V. Sahani, Reducing body CT radiation dose: beyond just changing the numbers, Am. J. Roentgenol. 201 (1) (2013) 33–40.
[10] A.R. Goldman, P.D. Maldjian, Reducing radiation dose in body CT: a practical approach to optimizing CT protocols, Am. J. Roentgenol. 200 (4) (2013) 748–754.
[11] C.H. McCollough, A.N. Primak, N. Braun, J. Kofler, L. Yu, J. Christner, Strategies for reducing radiation dose in CT, Radiol. Clin. 47 (1) (2009) 27–40.
[12] Y. Funama, K. Awai, O. Miyazaki, Y. Nakayama, T. Goto, Y. Omi, T. Shimonobo, D. Liu, Y. Yamashita, S. Hori, Improvement of low-contrast detectability in low-dose hepatic multidetector computed tomography using a novel adaptive filter: evaluation with a computer-simulated liver including tumors, Invest. Radiol. 41 (1) (2006) 1–7.
[13] M.K. Kalra, M.M. Maher, M.A. Blake, B.C. Lucey, K. Karau, T.L. Toth, G. Avinash, E.F. Halpern, S. Saini, Detection and characterization of lesions on low-radiation-dose abdominal CT images postprocessed with noise reduction filters, Radiology 232 (3) (2004) 791–797.
[14] S.T. Schindera, D. Odedra, S.A. Raza, T.K. Kim, H.-J. Jang, Z. Szucs-Farkas, P. Rogalla, Iterative reconstruction algorithm for CT: can radiation dose Be decreased while low-contrast detectability is preserved? Radiology 269 (2) (2013) 511–518.
[15] E.C. Ehman, L. Yu, A. Manduca, A.K. Hara, M.M. Shiung, D. Jondal, D.S. Lake, R.G. Paden, D.J. Blezek, M.R. Bruesewitz, C.H. McCollough, D.M. Hough, J.G. Fletcher, Methods for clinical evaluation of noise reduction techniques in abdominopelvic CT, Radiographics 34 (4) (2014) 849–862.
[16] N.K. Lee, S. Kim, S.B. Hong, T.U. Kim, H. Ryu, J.W. Lee, J.Y. Kim, Low-dose CT with the adaptive statistical iterative reconstruction V technique in abdominal organ injury: comparison with routine-dose CT with filtered back projection, Am. J. Roentgenol. 213 (3) (2019) 659–666.

[17] D. Marin, R.C. Nelson, S.T. Schindera, S. Richard, R.S. Youngblood, T.T. Yoshizumi, E. Samei, Low-tube-voltage, high-tube-current multidetector abdominal CT: improved image quality and decreased radiation dose with adaptive statistical iterative reconstruction algorithm–initial clinical experience, Radiology 254 (1) (2010) 145–153.

[18] A.K. Hara, R.G. Paden, A.C. Silva, J.L. Kujak, H.J. Lawder, W. Pavlicek, Iterative reconstruction technique for reducing body radiation dose at CT: feasibility study, Am. J. Roentgenol. 193 (3) (2009) 764–771.

[19] Z. Deák, J.M. Grimm, M. Treitl, L.L. Geyer, U. Linsenmaier, M. Körner, M.F. Reiser, S. Wirth, Filtered back projection, adaptive statistical iterative reconstruction, and a model-based iterative reconstruction in abdominal CT: an experimental clinical study, Radiology 266 (1) (2013) 197–206.

[20] S. Singh, M.K. Kalra, J. Hsieh, P.E. Licato, S. Do, H.H. Pien, M.A. Blake, Abdominal CT: comparison of adaptive statistical iterative and filtered back projection reconstruction techniques, Radiology 257 (2) (2010) 373–383.

[21] A. Gervaise, B. Osemont, S. Lecocq, A. Noel, E. Micard, J. Felblinger, A. Blum, CT image quality improvement using Adaptive Iterative Dose Reduction with wide-volume acquisition on 320-detector CT, Eur. Radiol. 22 (2) (2012) 295–301.

[22] P.B. Noël, S. Engels, T. Köhler, D. Muenzel, D. Franz, M. Rasper, E.J. Rummeny, M. Dobritz, A.A. Fingerle, Evaluation of an iterative model-based CT reconstruction algorithm by intra-patient comparison of standard and ultra-low-dose examinations, Acta Radiol. 59 (10) (2018) 1225–1231.

[23] A. Mileto, L.S. Guimaraes, C.H. McCollough, J.G. Fletcher, L. Yu, State of the art in abdominal CT: the limits of iterative reconstruction algorithms, Radiology 293 (3) (2019) 491–503.

[24] Y.J. Shin, W. Chang, J.C. Ye, E. Kang, D.Y. Oh, Y.J. Lee, J.H. Park, Y.H. Kim, Low-dose abdominal CT using a deep learning-based denoising algorithm: a comparison with CT reconstructed with filtered back projection or iterative reconstruction algorithm, Korean J. Radiol. 21 (3) (2020) 356–364.

[25] Y. Nakamura, T. Higaki, F. Tatsugami, J. Zhou, Z. Yu, N. Akino, Y. Ito, M. Iida, K. Awai, Deep learning–based CT image reconstruction: initial evaluation targeting hypovascular hepatic metastases, Radiology: Artif. Intell. 1 (6) (2019) e180011.

[26] C.M. McLeavy, M.H. Chunara, R.J. Gravell, A. Rauf, A. Cushnie, C. Staley Talbot, R.M. Hawkins, The future of CT: deep learning reconstruction, Clin. Radiol. 76 (6) (2021) 407–415.

[27] Y. Noda, T. Kaga, N. Kawai, T. Miyoshi, H. Kawada, F. Hyodo, A. Kambadakone, M. Matsuo, Low-dose whole-body CT using deep learning image reconstruction: image quality and lesion detection, Br. J. Radiol. 94 (1121) (2021) 20201329.

[28] M. Akagi, Y. Nakamura, T. Higaki, K. Narita, Y. Honda, J. Zhou, Z. Yu, N. Akino, K. Awai, Deep learning reconstruction improves image quality of abdominal ultra-high-resolution CT, Eur. Radiol. 29 (11) (2019) 6163–6171.

[29] C. Arndt, F. Güttler, A. Heinrich, F. Bürckenmeyer, I. Diamantis, U. Teichgräber, Deep learning CT image reconstruction in clinical practice, Röfo 193 (3) (2021) 252–261.

[30] C.T. Jensen, X. Liu, E.P. Tamm, A.G. Chandler, J. Sun, A.C. Morani, S. Javadi, N.A. Wagner-Bartak, Image quality assessment of abdominal CT by use of new deep learning image reconstruction: initial experience, AJR Am. J. Roentgenol. 215 (1) (2020) 50–57.

[31] T. Njølstad, A. Schulz, J.C. Godt, H.M. Brøgger, C.K. Johansen, H.K. Andersen, A.C.T. Martinsen, Improved image quality in abdominal computed tomography reconstructed with a novel Deep Learning Image Reconstruction technique - initial clinical experience, Acta Radiol. Open 10 (4) (2021) 20584601211008391.

[32] J. Solomon, P. Lyu, D. Marin, E. Samei, Noise and spatial resolution properties of a commercially available deep learning-based CT reconstruction algorithm, Med. Phys. 47 (9) (2020) 3961–3971.

[33] M. Nagata, Y. Ichikawa, K. Domae, K. Yoshikawa, Y. Kanii, A. Yamazaki, N. Nagasawa, M. Ishida, H. Sakuma, Application of deep learning-based denoising technique for radiation dose reduction in dynamic abdominal CT: comparison with standard-dose CT using hybrid iterative reconstruction method, J. Digit. Imag. 36 (4) (2023) 1578–1587.

[34] A. Tamura, E. Mukaida, Y. Ota, M. Kamata, S. Abe, K. Yoshioka, Superior objective and subjective image quality of deep learning reconstruction for low-dose abdominal CT imaging in comparison with model-based iterative reconstruction and filtered back projection, Br. J. Radiol. 94 (1123) (2021) 20201357.

[35] M.A. Shehata, A.M. Saad, S. Kamel, N. Stanietzky, A.M. Roman-Colon, A.C. Morani, K.M. Elsayes, C.T. Jensen, Deep-learning CT reconstruction in clinical scans of the abdomen: a systematic review and meta-analysis, Abdom Radiol (NY) 48 (8) (2023) 2724–2756.

[36] P. Schober, C. Boer, L.A. Schwarte, Correlation coefficients: appropriate use and interpretation, Anesth. Analg. 126 (5) (2018) 1763–1768.

[37] L. Cao, X. Liu, J. Li, T. Qu, L. Chen, Y. Cheng, J. Hu, J. Sun, J. Guo, A study of using a deep learning image reconstruction to improve the image quality of extremely low-dose contrast-enhanced abdominal CT for patients with hepatic lesions, Br. J. Radiol. 94 (1118) (2021) 20201086.

[38] J. Park, J. Shin, I.K. Min, H. Bae, Y.E. Kim, Y.E. Chung, Image quality and lesion detectability of lower-dose abdominopelvic CT obtained using deep learning image reconstruction, Korean J. Radiol. 23 (4) (2022) 402–412.

[39] J.G. Nam, J.H. Hong, D.S. Kim, J. Oh, J.M. Goo, Deep learning reconstruction for contrast-enhanced CT of the upper abdomen: similar image quality with lower radiation dose in direct comparison with iterative reconstruction, Eur. Radiol. 31 (8) (2021) 5533–5543.

[40] D.H. Lee, J.M. Lee, C.H. Lee, S. Afat, A. Othman, Image quality and diagnostic performance of low-dose liver CT with deep learning reconstruction versus standard-dose CT, Radiol Artif Intell 6 (2) (2024) e230192.

[41] S. Park, J.H. Yoon, I. Joo, M.H. Yu, J.H. Kim, J. Park, S.W. Kim, S. Han, C. Ahn, J.H. Kim, J.M. Lee, Image quality in liver CT: low-dose deep learning vs standard-dose model-based iterative reconstructions, Eur. Radiol. 32 (5) (2022) 2865–2874.

[42] P. Lyu, N. Liu, B. Harrawood, J. Solomon, H. Wang, Y. Chen, F. Rigiroli, Y. Ding, F.R. Schwartz, H. Jiang, C. Lowry, L. Wang, E. Samei, J. Gao, D. Marin, Is it possible to use low-dose deep learning reconstruction for the detection of liver metastases on CT routinely? Eur. Radiol. 33 (3) (2023) 1629–1640.

[43] C.T. Jensen, S. Gupta, M.M. Saleh, X. Liu, V.K. Wong, U. Salem, W. Qiao, E. Samei, N.A. Wagner-Bartak, Reduced-dose deep learning reconstruction for abdominal CT of liver metastases, Radiology 303 (1) (2022) 90–98.

[44] J. Hsieh, E. Liu, B. Nett, J. Tang, J.-B. Thibault, S. Sahney, A new era of image reconstruction: TrueFidelity[TM]. Technical White Paper on Deep Learning Image Reconstruction, 2019.

[45] S. Yang, Y. Bie, G. Pang, X. Li, K. Zhao, C. Zhang, H. Zhong, Impact of novel deep learning image reconstruction algorithm on diagnosis of contrast-enhanced liver computed tomography imaging: comparing to adaptive statistical iterative reconstruction algorithm, J. X Ray Sci. Technol. 29 (6) (2021) 1009–1018.

[46] D. Caruso, D. De Santis, A. Del Gaudio, G. Guido, M. Zerunian, M. Polici, D. Valanzuolo, D. Pugliese, R. Persechino, A. Cremona, L. Barbato, A. Caloisi, E. Iannicelli, A. Laghi, Low-dose liver CT: image quality and diagnostic accuracy of deep learning image reconstruction algorithm, Eur. Radiol. 34 (4) (2024) 2384–2393.

[47] M.E. Telesmanich, C.T. Jensen, J.L. Enriquez, N.A. Wagner-Bartak, X. Liu, O. Le, W. Wei, A.G. Chandler, E.P. Tamm, Third version of vendor-specific model-based iterativereconstruction (Veo 3.0): evaluation of CT image quality in the abdomen using new noise reduction presets and varied slice optimization, Br. J. Radiol. 90 (1077) (2017) 20170188.

[48] C. Yang, W. Wang, D. Cui, J. Zhang, L. Liu, Y. Wang, W. Li, Deep learning image reconstruction algorithms in low-dose radiation abdominal computed tomography: assessment of image quality and lesion diagnostic confidence, Quant. Imag. Med. Surg. 13 (5) (2023) 3161–3173.

[49] D. Racine, F. Becce, A. Viry, P. Monnin, B. Thomsen, F.R. Verdun, D.C. Rotzinger, Task-based characterization of a deep learning image reconstruction and comparison with filtered back-projection and a partial model-based iterative reconstruction in abdominal CT: a phantom study, Phys. Med. 76 (2020) 28–37.

[50] P. Apisarnthanarak, S. Hongpinyo, K. Saysivanon, C. Boonma, S. Janpanich, P. Ketkan, K. Muangsomboon, W. Teerasamit, S. Pongpornsup, P. Saiviroonporn, Abdominal CT radiation dose reduction at Siriraj hospital (phase II), The ASEAN Journal of Radiology 21 (3) (2020) 5–24.

[51] K.W. Shaqdan, A.R. Kambadakone, P. Hahn, D.V. Sahani, Experience with iterative reconstruction techniques for abdominopelvic computed tomography in morbidly and super obese patients, J. Comput. Assist. Tomogr. 42 (1) (2018) 124–132.

[52] L.R. Carucci, Imaging obese patients: problems and solutions, Abdom. Imag. 38 (4) (2013) 630–646.

[53] M.J. Modica, K.M. Kanal, M.L. Gunn, The obese emergency patient: imaging challenges and solutions, Radiographics 31 (3) (2011) 811–823.